

# Generation of sub-three-cycle pulses at 53 MHz repetition rate via nonlinear compression in optical parametric oscillator

Lixin Yuan (苑莉薪)<sup>1,†</sup>, Yu Cai (蔡宇)<sup>1,†</sup>, Yuxi Chu (储玉喜)<sup>1,2</sup>, Jintao Fan (范锦涛)<sup>1\*</sup>, and Minglie Hu (胡明列)<sup>1\*\*</sup>

<sup>1</sup>Ultrafast Laser Laboratory, Key Laboratory of Opto-electronic Information Science and Technology of Ministry of Education, School of Precision Instruments and Opto-electronics Engineering, Tianjin University, Tianjin 300072, China

<sup>2</sup>Georgia Tech Shenzhen Institute (GTSI), Tianjin University, Shenzhen 518067, China

\*Corresponding author: [fanjintao@tju.edu.cn](mailto:fanjintao@tju.edu.cn)

\*\*Corresponding author: [huminglie@tju.edu.cn](mailto:huminglie@tju.edu.cn)

Received December 29, 2021 | Accepted February 18, 2022 | Posted Online March 10, 2022

We report an experimental generation of few-cycle pulses at 53 MHz repetition rate. Femtosecond pulses with pulse duration of 181 fs are firstly generated from an optical parametric oscillator (OPO). Then, the pulses are compressed to sub-three-cycle with a hybrid compressor composed of a commercial single-mode fiber and a pair of prisms, taking advantage of the tunability of the OPO and the numerical simulating of the nonlinear compression system. Our compressed optical pulses possess an ultrabroadband spectrum covering over 470 nm bandwidth (at  $-10$  dB), and the output intensity fluctuation of our system is less than 0.8%. These results show that our system can effectively generate few-cycle pulses at a repetition rate of tens of megahertz with excellent long-term stability, which could benefit future possible applications.

**Keywords:** nonlinear compression; few cycle pulse; optical parametric oscillator.

**DOI:** [10.3788/COL202220.051901](https://doi.org/10.3788/COL202220.051901)

## 1. Introduction

Few-cycle pulses have attracted much attention owing to their successful applications in such fields as sensing<sup>[1]</sup>, production of attosecond pulses<sup>[2]</sup>, generation of high harmonics<sup>[3]</sup>, extreme-ultraviolet pulse<sup>[4]</sup>, advancement of novel X-ray sources<sup>[5]</sup>, and frequency combs<sup>[6]</sup>. To date, systematic methods have been developed to achieve few-cycle pulses to meet specific application needs. The measurement of few-cycle pulses can be based on nonlinear intensity cross correlation and the spectrum or spectral interferometry<sup>[7,8]</sup>. Spectral broadening and pulse compression are fundamental processes required in the few-cycle pulse generation. Therefore, considering the limited gain bandwidth, most few-cycle techniques focus on high-power, high-energy lasers and nonlinear pulse compression systems. Noise like mode-locked lasers have the potential to output high-energy pulses<sup>[9]</sup>. The nonlinear media include multiplates, multipass cells, and gas-filled hollow core fibers that are based on self-phase modulation (SPM)<sup>[10–13]</sup>. However, the repetition rates of such systems are commonly limited to kilohertz.

Indeed, few-cycle systems at repetition rates in the range of several tens of megahertz are of great value in those scenarios that require a high signal-to-noise ratio, large statistics, and a high flux. In the past decades, Kerr-lens mode-locked

Ti:sapphire lasers, providing the shortest pulses with only 5 fs directly from the oscillator, remain the major workhorse of the research field due to the remarkable spectral bandwidth of this gain material<sup>[14]</sup>. However, water cooling is essential due to the unavoidable heat load in the laser crystal, hindering their further application. Recently, with careful dispersion management, optical parametric oscillators (OPOs)<sup>[15]</sup>, optical parametric amplifiers (OPAs)<sup>[16]</sup>, and novel Mamyshev fiber oscillators<sup>[17]</sup> can also directly produce few-cycle pulses. In either of these cases, the cavity configurations need to be designed with great care.

Apart from direct generation, another efficient way to reach the few-cycle regime is to utilize nonlinear pulse compression in a highly nonlinear fiber. In 2009, nonlinear compression in an Er laser amplifier to the two-cycle pulse regime at a central wavelength of 1.17  $\mu\text{m}$  was demonstrated<sup>[18]</sup>. Very recently, spectral broadening in Er laser systems and then compression to  $< 10$  fs have also been presented with a highly nonlinear fiber<sup>[19]</sup>. The major challenge in these systems is the design of the highly nonlinear fiber. The ultrabroad spectrum generation in the anomalous dispersion fiber involves complex soliton dynamics, some of which, like higher-order soliton fission, will undermine the pulse quality and spectral coherence. The SPM effect is the main

nonlinear process that will ensure the coherence of spectral broadening in a normal dispersion fiber<sup>[20,21]</sup>. Therefore, the generation of high-power, high-repetition-rate few-cycle laser pulses faces an ongoing challenge.

It is worth noting that OPOs are a kind of versatile and flexible seed source that produces ultrashort optical pulses with a tunable wavelength, pulse duration, and power<sup>[22,23]</sup>. Moreover, nonlinear pulse compression can benefit greatly from these parameters. In this Letter, we demonstrate nonlinear compression of 181 fs pulses from a femtosecond OPO to the sub-three-cycle regime in a commercially available highly nonlinear fiber. First, we use numerical simulations to show that the average power, central wavelength, and pulse duration affect nonlinear compression for finding proper experimental parameters. Then, by adjusting the experimental condition accordingly, an ultrabroad spectrum with a 10 dB spectral bandwidth of 476 nm is obtained inside a normal dispersion fiber (UHNA7, Nufern) when the injected OPO pulses are centered at 1502 nm. We achieve pulse duration down to 14.5 fs (2.9 cycles centered at 1502 nm) by not only adjusting the hybrid compressor composed of a commercial single-mode fiber (SMF, Corning) and a pair of prisms but also tuning the state of the OPO. In the case of a central wavelength at 1463 nm of the injection pulses, the compressed pulses have a pulse duration of 22 fs (4.5 cycles centered at 1463 nm). Our work achieves few-cycle pulse generation by using a commercially available fiber together with a tunable laser source, which may expand the application space of high-repetition-rate few-cycle pulses.

## 2. Experiment

The experimental setup is shown in Fig. 1(a). As shown in Fig. 1(b), the laser source used in our experiment is a home-made femtosecond OPO, which is pumped by a home-built  $\text{Yb}^{3+}$  fiber amplifier system with 2 W output power at 53 MHz repetition rate. A 3-mm-long, 12.3-mm-wide, and 1-mm-thick 5% MgO-doped periodically poled lithium niobate (MgO:PPLN) crystal, which contains ten gratings with periods ranging from 27.58 to 31.59  $\mu\text{m}$  in steps of 0.5  $\mu\text{m}$ , is used as the gain element in the OPO. The PPLN crystal is anti-reflection coated over 1000–1100 nm and 1420–2000 nm ( $R < 1\%$ ). The length of the linear cavity is set to be  $\sim 2.83$  m to ensure the synchronous pumping condition. The output pulses are injected into a commercial 27 cm UHNA7 fiber with a tiny core diameter of 2.4  $\mu\text{m}$  by lens  $L_1$  ( $f = 5.95$  mm). The group velocity dispersion (GVD) profile of the UHNA7 fiber is shown in Fig. 1(c)<sup>[24]</sup>. The normal dispersion broadening minimizes noise and ensures a clean phase accumulation that can be recompressed. For efficient pulse compression, we utilize a two-stage compression scheme. In the first stage, a 15 cm commercial SMF is directly spliced with the UHNA7 fiber, and the GVD profile of the SMF is shown in Fig. 1(c)<sup>[25]</sup>. For the follow-up compression stage, a pair of SF11 prisms is used where the pulse can be recompressed to shorter pulse duration. Last, an autocorrelator (PulseCheck-50, APE GmbH) is used to characterize the pulse duration.

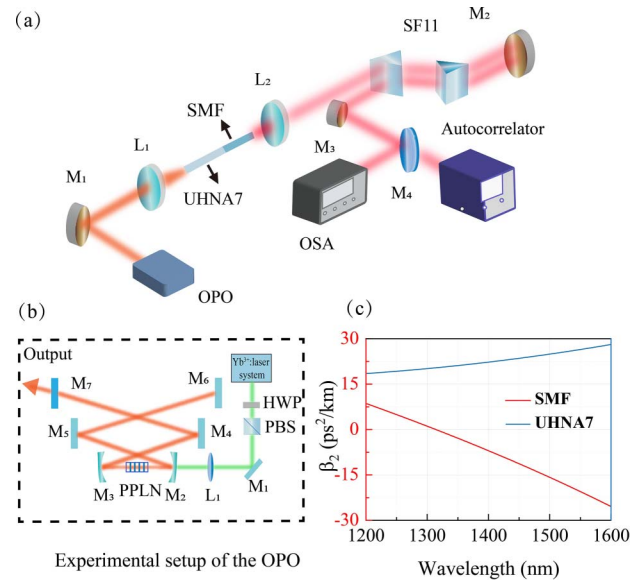


**Fig. 1.** (a) Schematic diagram of the experimental setup. M, mirrors; L, lenses; SF11, Brewster-angled prism pulse compressor; OSA, optical spectrum analyzer. (b) Experimental setup of the OPO. HWP, half-wave plate; PBS, polarizing beam splitter;  $M_1, M_4-M_7$ , mirrors;  $M_2, M_3$ , lenses; PPLN, periodically poled lithium niobate crystal. (c) The GVD ( $\beta_2$ ) profile of UHNA7 and SMF.

## 3. Experimental Results and Discussion

First, we conduct a numerical simulation of the nonlinear pulse compression process for injection pulses with different power, wavelength, and pulse duration. The injection parameters are taken from the measured OPO output in the experiment. A theoretical model based on the generalized nonlinear Schrödinger equation (GNLSE) is used to simulate the dynamics of pulse propagation in the UHNA7 and SMF<sup>[26]</sup>. We simulate the spectral broadening in the UHNA7 fiber and the dispersion compensation in a hybrid compressor composed of 15 cm SMF and a pair of SF11. In the simulation, the seed pulse is an ideal Gaussian pulse. The final compressed pulses can be obtained by adjusting the prisms. The Strehl ratio (SR) is an index to quantify how close the compressed pulse is compared to a transform-limited pulse with the same spectrum. SR is defined as<sup>[27]</sup>

$$\text{SR} = \frac{1/\int |A|^2 dt}{1/\int |A_{\text{TL}}|^2 dt}, \quad (1)$$

where  $|A|^2$  and  $|A_{\text{TL}}|^2$  are the normalized temporal envelopes of the compressed and transform-limited pulses, respectively. In Fig. 2(a), we present the simulated SR of compressed pulses with different input parameters. For different central wavelengths, pulse durations, and powers, the maximum value that the SR can reach is different. For a better understanding of this cube, we also show the results by fixing one of the parameters, and the results are shown in Figs. 2(b)–2(d). The reason for this phenomenon is that through the nonlinear compression system a change of the central wavelength, pulse duration, and power will

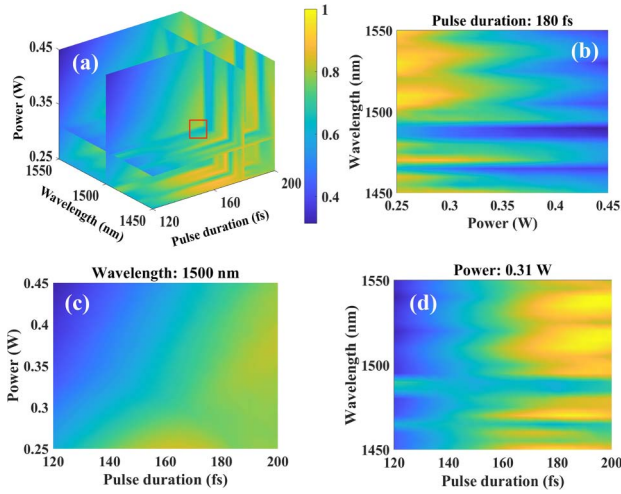


**Fig. 2.** (a) Simulation of SR for different wavelengths, pulse durations, and powers. (b)–(d) Slice diagrams of (a) with pulse duration of 180 fs, central wavelength of 1500 nm, and power of 0.31 W, respectively. The color bar represents the SR.

lead to a change of the accumulated nonlinear chirp and higher-order dispersion.

Here, we use a synchronously pumped femtosecond OPO, whose output pulse duration, wavelength, and power are strongly correlated with each other due to the intracavity group delay dispersion and nonlinear effects. Therefore, the OPO output pulses cannot cover all points in the simulation cube. We experimentally observe the compressed pulses with the shortest duration when the input OPO pulses have a pulse duration of 181 fs and a central wavelength of 1502 nm. The spectral bandwidth of the OPO is 24 nm (at  $-3$  dB), and the output average power is 620 mW. The measured spectrum (with spectrum analyzer Yokogawa, AQ6374) and autocorrelation results are shown in Figs. 3(a) and 3(b). Compared to the simulation result, we find that the SR result at our experimental condition is relatively closer to one than that of the surrounding area [labeled with a red square mark in Fig. 2(a)], indicating that the compressed pulses have a better quality.

To better describe pulse propagation in the 27 cm UHNA7 fiber and the 15 cm SMF, Fig. 4(b) shows the spectral evolution

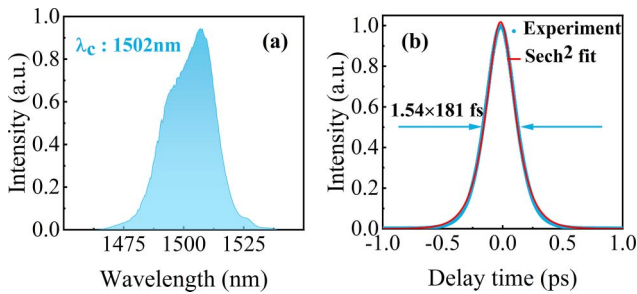


**Fig. 3.** (a) Output spectrum from the OPO. (b) Typical intensity autocorrelation trace at 1502 nm.

during pulse propagation. Below the white dashed line, the pulse propagates in the UHNA7 fiber where the spectrum begins broadening. It can be seen from the simulation that the spectral width hardly broadens as the transmission distance of the pulse in the UHNA7 increases. In order to ensure enough spectral broadening and avoid the accumulation of more nonlinear chirps due to a too long fiber, the UHNA7 fiber with a length of 27 cm was used in the experiment. In the wavelength range of normal dispersion, the main reason for spectral broadening is SPM and optical wave breaking<sup>[20,21]</sup>. In the initial stage of spectral broadening, SPM plays a major role, and afterward the spectrum further broadens under the effect of optical wave breaking. The model based on the GNLS yields good agreement with our experimental measurements in Fig. 4(a). The bandwidth of the experimental spectrum is 476 nm (at  $-10$  dB level) at a launched pulse power of 620 mW (11.7 nJ). The output power is 102 mW, yielding  $\sim 16.5\%$  efficiency due to the lens coupling loss, splicing loss, and nonlinear spectral broadening loss.

After that, the pulses are injected into the 15 cm SMF above the white dotted line in Fig. 4(b) where the spectrum is no longer broadened. The pulses are only compressed in the time domain without the effects of higher-order soliton fission and Raman soliton self-frequency shift. The phenomenon happens because the length of the SMF is short, and the negative dispersion provided by the SMF is not enough to compensate the positive chirp provided by the UHNA7 fiber. Thus, the 15 cm SMF is selected as the pre-compression in the experiment.

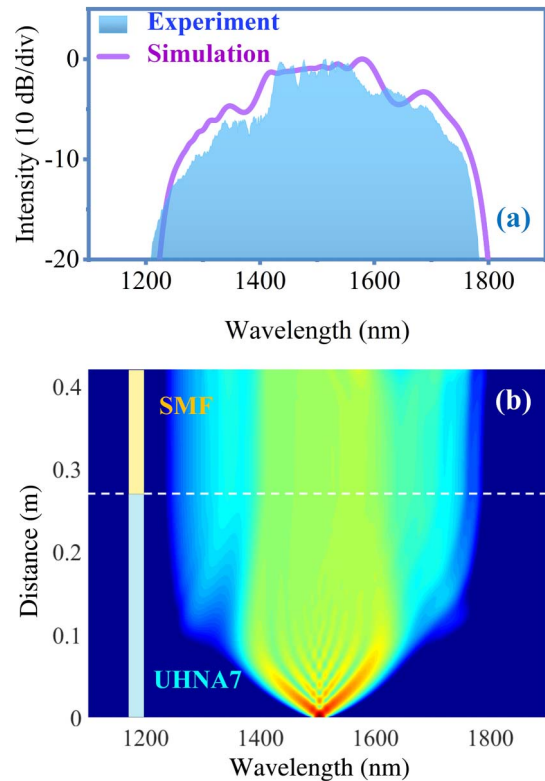


**Fig. 4.** (a) Experimental and simulated final output spectra at 1502 nm. (b) Simulation of spectral evolution in 27 cm UHNA7 and 15 cm SMF.



After passing the UHNA7 and SMF, the pulses are recompressed by the SF11 prism. This fiber–prism hybrid compression system can bring the following advantages: (1) the prisms can precisely compensate the second-order dispersion, thus leading to shorter pulse duration, and (2) the fiber can make the system more compact. Since the second-order dispersion of the prisms is limited, quite a long distance between the prisms is required if only prisms were used. After compression, the interferometric autocorrelation traces of the pulse in accord with the ratio of 8:1 are shown in Fig. 5(a). The intensity envelope and temporal phase of the pulse retrieved from the phase and intensity from correlation and spectrum only (PICASO) algorithm<sup>[7]</sup> are shown in Fig. 5(b), which reveals a high-quality 14.5 fs pulse corresponding to nearly 2.9 optical cycles at the center wavelength of 1502 nm. The measured pulse duration is slightly longer than the transform-limited one ( $\sim 10$  fs) owing to the residual higher-order dispersion and nonlinearity. The recorded output power of the compressed pulses is 66 mW.

To investigate the long-term stability of the few-cycle pulses, a spectrometer covering a wavelength range of 900 nm to 1700 nm is used to measure the spectrum within 20 min, as shown in the inset in Fig. 5(c). The root-mean-square (RMS) of the spectral intensity at 1502 nm is 0.98% (the orange trace). The blue line in Fig. 5(c) shows the change of 10 dB spectral bandwidth, presenting 0.78% RMS, indicating that the spectral bandwidth has good stability within the same time span. In the experiment, the whole system is exposed in free space. Given that the whole system is packaged and isolated in a closed box to reduce the environmental disturbance, the stability of the system can be further

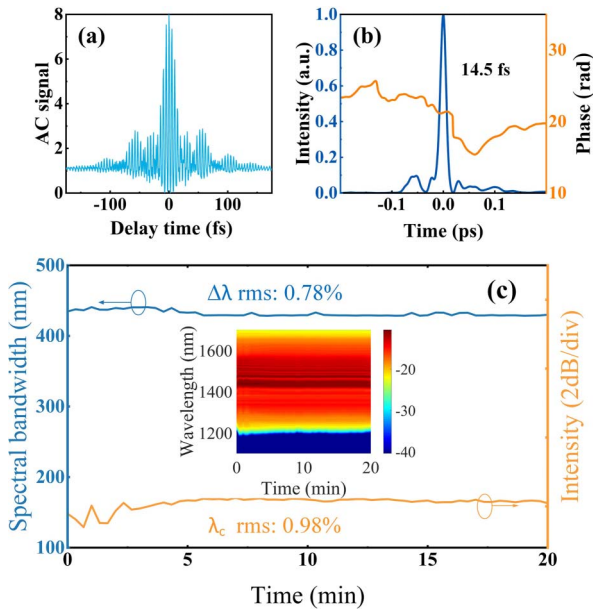


**Fig. 5.** (a) Interferometric autocorrelation of pulses at 1502 nm; AC signal, autocorrelation signal. (b) Temporal intensity envelope and phase at 1502 nm. (c) Central wavelength and spectral bandwidth (at  $-10$  dB) stability at 1502 nm over a period of 20 min. The inset shows spectral stability measurement over the same period.

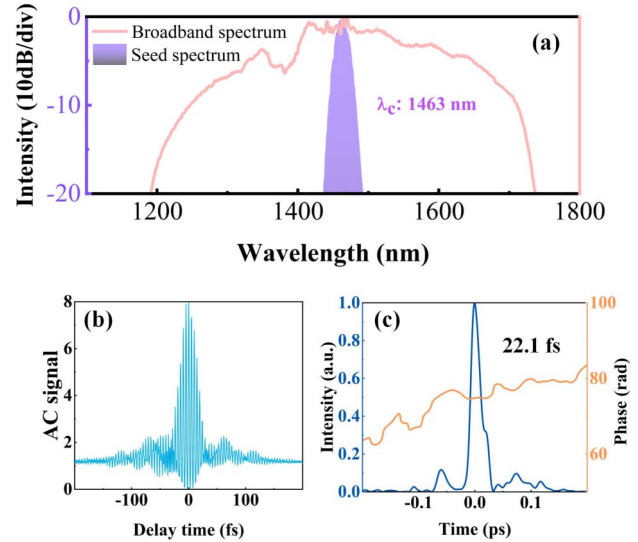


**Fig. 6.** (a) Ultrabroad spectrum after the UHNA7 fiber and seed spectrum. (b) Interferometric autocorrelation of the pulses at 1463 nm after OPO adjustment. (c) Temporal intensity envelope and phase at 1463 nm after OPO adjustment.

improved. Overall, the system has excellent stability, which provides a basis for subsequent generation of few-cycle pulses and ensures their stability.

Adjusting the period of the OPO crystal will get few-cycle pulses at different center wavelengths. In another case, 22.1 fs pulses are generated. The OPO output pulses are centered at a wavelength of 1463 nm [see purple-filled part in Fig. 6(a)], and the spectral bandwidth is 33 nm (at  $-3$  dB). The pulse duration is 140 fs, and the average output power is 452 mW (8.5 nJ). The broadened spectrum from the UHNA7 fiber is shown as the pink line in Fig. 6(a). As shown in Fig. 6(b), the interferometric autocorrelation traces are obtained after the pulses are compressed by the SMF and prism sequence. Similarly, the intensity envelope and temporal phase of the pulses retrieved from PICASO are shown in Fig. 6(c). In brief, 22.1 fs pulses can be obtained that correspond to 4.5 optical cycles at a central wavelength of 1463 nm after tuning the source. The average output power is 46 mW after pulse compression. Because the state of the OPO changes, resulting in the change of dispersion and nonlinearity in the nonlinear compression system, the compressed pulse duration is slightly longer than in the previous state.

## 4. Conclusion

In summary, a simple and efficient nonlinear compression system that can produce high-quality and high-repetition-rate sub-three-cycle pulses is demonstrated. Benefitting from the tuning ability of the femtosecond OPO, the nonlinear compression evolution process can be optimized, and, in this way, we have obtained 66 mW, 14.5 fs pulses (2.9 optical cycles at 1502 nm). The simple two-stage compressor composed of an SMF and a pair of prisms makes pulse compression not only

compact but also sufficient. Significantly, the highly nonlinear fiber for spectral broadening and the SMF for pulse compressing are both common commercial fibers without cumbersome structures. In addition, our spectral stability measurement indicates that the system is reliable. Our work thus provides a new and useful method for few-cycle pulse generation using only commercially available systems, which will facilitate applications that demand ultrashort pulses at a high repetition rate.

Besides, high-quality few-cycle pulse generation is dominated by the achieved broadest spectrum and dispersion compensation. Thus, the dispersion profiles of the UHNA7 and SMF play a key role in our system, resulting in the upper limit of the proposed method. However, taking advantage of the tunable laser source, only by changing the nonlinear fiber and the corresponding compressor, our method can be readily utilized at other wavelength regions.

## Acknowledgement

This work was supported by the National Natural Science Foundation of China (NSFC) (Nos. 61827821 and 62105237) and the Research and Development Program in Key Areas of Guangdong Province, China (No. 2020B090922004).

†These authors contributed equally to this work.

## References

1. C. M. Jewart, Q. Wang, J. Canning, D. Grobnc, S. J. Mihailov, and K. P. Chen, "Ultrafast femtosecond-laser-induced fiber Bragg gratings in air hole microstructured fibers for high-temperature pressure sensing," *Opt. Lett.* **35**, 1443 (2010).
2. S.-W. Huang, G. Cirmi, J. Moses, K.-H. Hong, S. Bhardwaj, J. R. Birge, L.-J. Chen, E. Li, B. J. Eggleton, G. Cerullo, and F. X. Kärtner, "High-energy pulse synthesis with sub-cycle waveform control for strong-field physics," *Nat. Photonics* **5**, 475 (2011).
3. O. D. Mücke, "Isolated high-order harmonics pulse from two-color-driven Bloch oscillations in bulk semiconductors," *Phys. Rev. B* **84**, 081202 (2011).
4. Y. Jia, L. Guo, S. Hu, X. Jia, D. Fan, R. Lu, S. Han, and J. Chen, "Time-energy analysis of the photoionization process in a double-XUV pulse combined with a few-cycle IR field," *Chin. Opt. Lett.* **19**, 123201 (2021).
5. C. Spielmann, N. H. Burnett, S. Sartania, R. Koppitsch, M. Schnürer, C. Kan, M. Lenzner, P. Wobrauschek, and F. Krausz, "Generation of coherent X-rays in the water window using 5-femtosecond laser pulses," *Science* **278**, 661 (1997).
6. A. J. Lind, A. Kowligy, H. Timmers, F. C. Cruz, N. Nader, M. C. Silfies, T. K. Allison, and S. A. Diddams, "Mid-infrared frequency comb generation and spectroscopy with few-cycle pulses and  $\chi^{(2)}$  nonlinear optics," *Phys. Rev. Lett.* **124**, 133904 (2020).
7. J. W. Nicholson, J. Jasapara, W. Rudolph, F. G. Omenetto, and A. J. Taylor, "Full-field characterization of femtosecond pulses by spectrum and cross-correlation measurements," *Opt. Lett.* **24**, 1774 (1999).
8. Z. Si, X. Shen, J. Zhu, L. Lin, L. Bai, and J. Liu, "All-reflective self-referenced spectral interferometry for single-shot measurement of few-cycle femtosecond pulses in a broadband spectral range," *Chin. Opt. Lett.* **18**, 021202 (2020).
9. Z. Zhang, J. Tian, C. Xu, R. Xu, Y. Cui, B. Zhuang, and Y. Song, "Noise-like pulse with a 690 fs pedestal generated from a nonlinear Yb-doped fiber amplification system," *Chin. Opt. Lett.* **18**, 121403 (2020).
10. M. Seo, K. Tsendsuren, S. Mitra, M. Kling, and D. Kim, "High-contrast, intense single-cycle pulses from an all thin-solid-plate setup," *Opt. Lett.* **45**, 367 (2020).
11. M. Kaumanns, V. Pervak, D. Kormin, V. Leshchenko, A. Kessel, M. Ueffing, Y. Chen, and T. Nubbemeyer, "Multipass spectral broadening of 18 mJ pulses compressible from 13 ps to 41 fs," *Opt. Lett.* **43**, 5877 (2018).
12. J. Song, Z. Wang, X. Wang, R. Lü, H. Teng, J. Zhu, and Z. Wei, "Generation of 601 fs pulse from an 8 kHz Nd:YVO<sub>4</sub> picosecond laser by multi-pass-cell spectral broadening," *Chin. Opt. Lett.* **19**, 093201 (2021).
13. S. Bohman, A. Suda, T. Kanai, S. Yamaguchi, and K. Midorikawa, "Generation of 5.0 fs, 5.0 mJ pulses at 1 kHz using hollow-fiber pulse compression," *Opt. Lett.* **35**, 1887 (2010).
14. R. Ell, U. Morgner, F. X. Kärtner, J. G. Fujimoto, E. P. Ippen, V. Scheuer, G. Angelow, T. Tschudi, M. J. Lederer, A. Boiko, and B. Luther-Davies, "Generation of 5-fs pulses and octave-spanning spectra directly from a Ti:sapphire laser," *Opt. Lett.* **26**, 373 (2001).
15. R. A. McCracken and D. T. Reid, "Few-cycle near-infrared pulses from a degenerate 1 GHz optical parametric oscillator," *Opt. Lett.* **40**, 4102 (2015).
16. Z. Hong, Q. Zhang, S. A. Rezvani, P. Lan, and P. Lu, "Tunable few-cycle pulses from a dual-chirped optical parametric amplifier pumped by broadband laser," *Opt. Laser Technol.* **98**, 169 (2018).
17. C. Ma, A. Khanolkar, Y. Zang, and A. Chong, "Ultrabroadband, few-cycle pulses directly from a Mamyshev fiber oscillator," *Photonics Res.* **8**, 65 (2020).
18. A. Sell, G. Krauss, R. Scheu, R. Huber, and A. Leitenstorfer, "8-fs pulses from a compact Er:fiber system: quantitative modeling and experimental implementation," *Opt. Express* **17**, 1070 (2009).
19. D. M. Lesko, H. Timmers, S. Xing, A. Kowligy, A. J. Lind, and S. A. Diddams, "A six-octave optical frequency comb from a scalable few-cycle erbium fibre laser," *Nat. Photonics* **15**, 281 (2021).
20. C. Finot, B. Kibler, L. Provost, and S. Wabnitz, "Beneficial impact of wave-breaking for coherent continuum formation in normally dispersive nonlinear fibers," *J. Opt. Soc. Am. B* **25**, 1938 (2008).
21. L. E. Hooper, P. J. Mosley, A. C. Muir, W. J. Wadsworth, and J. C. Knight, "Coherent supercontinuum generation in photonic crystal fiber with all-normal group velocity dispersion," *Opt. Express* **19**, 4902 (2011).
22. H. Kong, J. Bian, J. Yao, Q. Ye, and X. Sun, "Temperature tuning of BaGa<sub>4</sub>Se<sub>7</sub> optical parametric oscillator," *Chin. Opt. Lett.* **19**, 021901 (2021).
23. J. Song, X. Meng, Z. Wang, X. Wang, W. Tian, J. Zhu, S. Fang, H. Teng, and Z. Wei, "Harmonically pump a femtosecond optical parametric oscillator to 1.13 GHz by a femtosecond 515 nm laser," *Chin. Opt. Lett.* **18**, 033201 (2020).
24. P. Ciąćka, A. Rampur, A. Heidt, T. Feurer, and M. Klimczak, "Dispersion measurement of ultra-high numerical aperture fibers covering thulium, holmium, and erbium emission wavelengths," *J. Opt. Soc. Am. B* **35**, 1301 (2018).
25. Corning, "Corning SMF-28e+ optical fiber product information," <https://www.corning.com/media/worldwide/coc/documents/Fiber/PI-1463-AEN.pdf> (2022).
26. J. M. Dudley and J. R. Taylor, *Supercontinuum Generation in Optical Fibers* (Cambridge University, 2010).
27. S. Wang, B. Liu, M. Hu, and C. Wang, "On the efficiency of parabolic self-similar pulse evolution in fiber amplifiers with gain shaping," *J. Lightwave Technol.* **34**, 3023 (2016).